# Flash Photolysis of Trimethylantimony and Trimethylbismuth and the Quenching of Excited Antimony and Bismuth Atoms

J. Connor, P. J. Young, and O. P. Strausz*

*Contribution from the Department of Chemistry,
University of Alberta, Edmonton, Alberta, Canada. Received June 23, 1970*

**Abstract:** The flash photolysis of $Sb(CH_3)_3$ and $Bi(CH_3)_3$ has been studied by kinetic absorption spectroscopy and emission spectroscopy. Several excited states of the metal atoms were detected, together with band systems of $Sb_2$ and $Bi_2$. Several unidentified band systems, one of which is tentatively assigned to $BiCH_3$, were also observed. In the presence of $O_2$ or $CO_2$ in the $Bi(CH_3)_3$ system the spectrum of BiO appeared, indicating excited-bismuth-sensitized decomposition. Quenching studies were carried out with several gases and relative quenching efficiencies determined. An interesting observation is reported on the alteration of relative radiative transition probabilities from a given atomic level in induced emission as compared to spontaneous emission.

The transfer of electronic excitation energy is of inherent interest in photochemistry and of practical importance in the study of photosensitization reactions. Molecular photosensitization has been investigated in considerable depth[1] both from a mechanistic and a synthetic viewpoint, but little is known concerning energy transfer from atomic species. Even the quenching of excited mercury,[2] the subject of the earliest and the most extensive study, is not yet well understood. Other atomic systems which have been investigated include cadmium,[3,4] alkali metals,[5] arsenic,[6] oxygen,[7] thallium,[8] and lead.[9] Spin–orbit relaxation of iodine,[10] selenium,[11] iron,[12] and arsenic[6] has also been studied, but in these cases the amount of energy to be transferred is rather small (<1 eV) and the factors governing relaxation are somewhat different.

Recent experiments in this laboratory[4] have shown that volatile alkylmetal compounds provide a useful flash-photolytic source of metal atoms. We have used this technique to produce excited antimony and bismuth atoms in an attempt to extend the limited amount of data available on electronic energy transfer from excited atomic species and to investigate some of the more important processes occurring in collisions of excited atoms with molecules.

## Experimental Section

A conventional flash-photolysis apparatus, with a 75-cm long quartz flash lamp and reactions cell, was employed. Spectra were recorded with Hilger medium or large quartz spectrographs on Kodak 103a-O plates sensitized for the far-uv by sodium salicylate and developed for 3.5 min in Kodak D19 developer. Numerical data were obtained by plate photometry employing a Joyce, Loebl Mark III recording microdensitometer.

Experiments were carried out both in absorption and emission. In order to convert emission peak heights, obtained by plate photometry, into relative concentrations, it is necessary to determine the relationship between the intensity of light falling on the photographic plate and the optical density change it produces. The intensity, $I$, of the output of a spectroscopic flash lamp was varied by inserting a calibrated rhodium step filter into the light path. The plate densities produced in this way in the wavelength region 2900–3100 Å on the medium quartz spectrograph and 2500–3300 Å on the large quartz spectrograph were measured and plotted against log $I/I_0$, where $I_0$ = intensity with no filter. The plots were linear in the density range 0.2–1.4. The slope, $\gamma$, varied somewhat from plate to plate, with wavelength and with development conditions, but was given by $\gamma = (0.77 \pm 0.10)$ $D$ unit for the medium quartz spectrograph and $\gamma = 0.6$ $D$ unit at 3267 Å, $\gamma = 0.3$ $D$ unit at 2428 Å for the large quartz spectrograph.

To ensure that the base of all emission lines fell in the linear region of plate sensitivity, all plates for emission work were pre-exposed to a shaded white light so as to produce a background plate density of about 0.2 $D$ unit. Under these conditions the change in plate density, $\Delta D_n$, produced by emission of intensity $I_n$ from a species of concentration $C_n$, is given by

$$\Delta D_n = \gamma \log (I_n + I')/I'$$

where $I'$ is the intensity of the background fogging radiation. Hence

$$\frac{I_n}{I_m} = \frac{10^{\Delta D_n/\gamma} - 1}{10^{\Delta D_m/\gamma} - 1} = \frac{C_n}{C_m}$$

Two assumptions are implicit in this derivation: firstly, that the effects of the plate of exposure to diffuse white light and to sharp atomic emissions are simply additive and, secondly, that the emission intensities are not distorted by spectrograph slit effects in the same way as atomic absorption intensities are. Half-path experiments to test this last assumption are not feasible since the emitted light reaching the photographic plate does not come with uniform distribution from all parts of the reaction vessel.

A few time-resolved emission experiments were carried out by replacing the plate holder on the medium quartz spectrograph by a Hilger and Watts E720 photomultiplier and scanning unit. The instrument was calibrated with respect to wavelength by scanning the outputs of Hg, Zn, and Cd lamps. It was then possible to display output signals (*i.e.*, emission intensities) at a particular wavelength as a function of time on an oscilloscope.

Trimethylantimony (TMSb) and trimethylbismuth (TMBi) were supplied by Alfa Inorganics Inc. and, after repeated pump–thaw–freeze cycling, were used without further purification. Argon was analyzed as Ar, 99.8%; $N_2$, 0.13%; $O_2$, 0.09%; $H_2O$ < 10 ppm, and was used without purification. $CO_2$, $H_2$, $O_2$, $N_2$, CO, and Xe were Airco assayed reagent grade supplied with analyses indicating negligible impurity. Ethylene and ethane were Phillips research grade, 99.9 and 99.92 mol % purity, respectively, and were used without further purification. Methane was Matheson research

(1) J. G. Calvert and J. N. Pitts, "Photochemistry," Wiley, New York, N. Y., 1966, p 543.

(2) R. J. Cvetanović, *Progr. React. Kinet.*, 2, 39 (1964); H. E. Gunning and O. P. Strausz, *Advan. Photochem.*, 4, 143 (1966).

(3) S. Tsunashima, S. Satoh, and S. Sato, *Bull. Chem. Soc. Jap.*, 42, 329 (1969).

(4) P. J. Young, G. Greig, and O. P. Strausz, *J. Amer. Chem. Soc.*, 92, 413 (1970).

(5) D. R. Jenkins, *Proc. Roy. Soc., Ser. A*, 293, 493 (1966).

(6) A. B. Callear and R. J. Oldman, *Trans. Faraday Soc.*, 64, 840 (1968).

(7) S. V. Filseth, F. Stuhl, and K. H. Welge, *J. Chem. Phys.*, 52, 239 (1970), and references therein.

(8) D. R. Jenkins, *Proc. Roy. Soc., Ser. A*, 303, 467 (1968).

(9) D. R. Jenkins, *ibid., Ser. A*, 313, 551 (1969).

(10) R. J. Donovan and D. Husain, *Trans. Faraday Soc.*, 62, 2023 (1966).

(11) A. B. Callear and W. J. R. Tyerman, *ibid.*, 62, 2313 (1966).

(12) A. B. Callear and R. J. Oldman, *ibid.*, 63, 2888 (1967).

**Table I.** Species Observed in Absorption in Flashed TMBi

| Species | Transition, Å | Conditions under which observed | Time to max intensity, μsec | Time species persists in system, μsec | Comments |
|---|---|---|---|---|---|
| Bi $^4S^0$ | $^4P_{1/2} \leftarrow 3068$ | All | 50 | 300 | Decay not simple first or second order |
| Bi $^2D_{3/2}^0$ | $^2P_{1/2} \leftarrow 2898$ | All | 20 | 100 | |
| Bi $^2D_{5/2}^0$ | $^2P_{3/2} \leftarrow 2938$ | All | 20 | 100 | Quenched by 100 Torr of $H_2$, $C_2H_4$ |
| Bi $^2P_{1/2}^0$ | $? \leftarrow 2730$ | All | 20 | 100 | |
| Bi$_2$ $X^1\Sigma_g^+$ | $B \leftarrow X$ 5000 | All | 150 | 500 | |
| Bi$_2$ $X^1\Sigma_g^+$ | $C \leftarrow X$ continuum around 3150 Å | TMBi > 0.1 Torr | 150 | 500 | |
| Bi$_2$ $X^1\Sigma_g^+$ | $D \leftarrow X$ around 2700 | All | 150 | 500 | |
| Bi$_2$ $X^1\Sigma_g^+$ | $? \leftarrow X$ 2100–2200 | All | 150 | 500 | Weak, complicated by overlap with other systems; not analyzed |
| CH$_3$ | 2160 | All | 30 | 100 | |
| ? | 2900–3100 | TMB > 0.1 Torr | 20 | 50 | See text |
| BiCH$_3$ (?) | 2490, 2555, 2615 | 2615 Å, all; others at TMBi > 5 × $10^{-2}$ Torr | 20 | See text | See text |
| ? | 2228, 2231 | All | 30 | 50 | Sharp; 2231 Å at least partly due to ground-state bismuth |
| ? | 2130, 2204 | TMBi–Ar, –CO$_2$, or –N$_2$; not in H$_2$, CH$_4$, or C$_2$H$_4$ | 30 | 150 | Weak, diffuse |
| BiO $X_1$ $^2\Pi_{1/2}$ | $A \leftarrow X_1$ (1, 0), (0, 0), and (0, 1) bands at 2541, 2591, and 2638, respectively | Added O$_2$, CO$_2$ (20 Torr) no $v'' = 1$ in CO$_2$) | 50 | >500 | |
| ? | 2290, 2330 3090, 3165 | Added CO$_2$ (20 Torr) | 20 | 70 | See text |

grade, minimum purity 99.8%, and was used without further purification.

For the emission work a mixture of different composition was required for each flash. Mixtures were prepared in a magnetically stirred glass mixing vessel with Teflon bearings.

## Results and Discussion

**(a) TMBi.** TMBi exhibits a broad absorption in the far-uv with a maximum at 2115 Å ($\epsilon$ 1.65 × $10^4$ l. mol$^{-1}$ cm$^{-1}$) and shoulders at 2225 ($\epsilon$ 1.4 × $10^4$) and 2600 Å ($\epsilon$ 2.4 × $10^3$). With quartz reaction cells, absorption took place in the entire region.

The flash photolysis (10 kV, 3000 J) of TMBi (1–10$^{-3}$ Torr) in the presence of argon (10–600 Torr) produces a variety of atomic and molecular species. The observations made are summarized in Table I. When the spectroscopic flash was not employed several atomic transitions were detected in emission. An energy level diagram for the Bi atom showing the states detected in emission and absorption is given in Figure 1.[13]

The 2900–3100-Å system observed at high TMBi pressures consists of an absorption, 100 Å wide, centered at 2935 Å, and a series of red degraded bands. Positions of the band heads and the splittings between bands are given in Table II. Although the spectrum appears to be typical of a heavy diatomic molecule, the rate of decay is much more rapid than that of ground-state Bi$_2$ and the frequency differences between successive bands are larger than the vibrational frequencies in any known excited state of Bi$_2$.[14] No assignment has been made.

The system assigned to BiCH$_3$ decays rapidly during the photolysis flash but after the flash persists for ~300 μsec. Flash energy variation studies at 100-μsec delay show that the intensity of the 2615-Å band decreases

(13) Nat. Bur. Stand. (U. S.), Circ., 467 (III), 219 (1958).
(14) G. Herzberg, "Spectra of Diatomic Molecules," Van Nostrand, Princeton, N. J., 1950.

**Table II.** 2900–3100-Å System Observed in Flashed TMBi

| λ, Å | $\nu$, cm$^{-1}$ | $\Delta\nu$, cm$^{-1}$ |
|---|---|---|
| 2922 | 34230 ± 10 | |
| | | 360 |
| 2953 | 33870 | |
| | | 210 |
| 2971 | 33660 | |
| | | 200 |
| (2989)[a] | 33460 | |
| | | 220 |
| 3008 | 33240 | |
| | | 220 |
| 3028 | 33020 | |
| | | 230 |
| 3049 | 32790 | |
| | | 200 |
| (3068)[a] | 32590 | |
| | | 230 |
| 3090 | 32360 | |
| | | 220 |
| 3111 | 32140 | |
| | | 180 |
| 3129 | 31960 | |
| | | 230 |
| 3152 | 31730 | |
| | | 210 |
| 3173 | 31520 | |

[a] Values in parentheses are uncertain because of overlap with intense atomic transitions.

with increasing energy, suggesting that the carrier is removed by photolysis. It is a reasonable assumption that BiCH$_3$ or, possibly, Bi(CH$_3$)$_2$ is the carrier.

The bands at 2290, 2330, 3090, and 3165 Å, which appear only with added CO$_2$, fall into two pairs, the splitting in each pair being 750 ± 20 cm$^{-1}$. A possible carrier is the previously unobserved X$_2$ $^2\Pi_{3/2}$ state of BiO, estimated by Bridge and Howell[15] to lie ~8000 cm$^{-1}$

(15) N. K. Bridge and H. G. Howell, Proc. Phys. Soc., 67, 44 (1954).
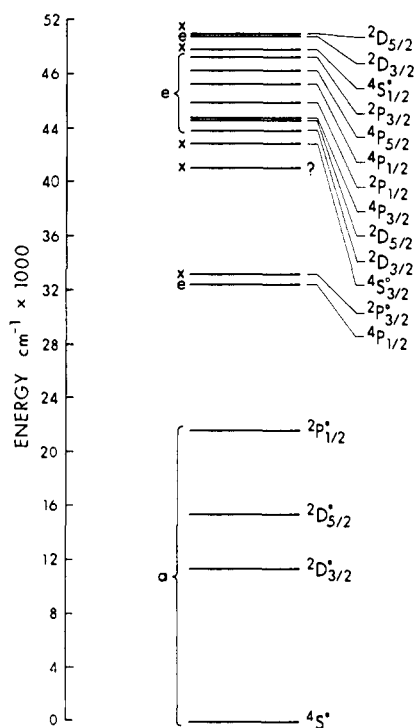
Figure 1. Atomic energy level diagram for bismuth: a, states observed in absorption; e, states observed in emission; x, not observed.



Figure 2. Emission from Bi(7s $^4P_{1/2}$) at 3068 Å: a, 100 Torr of Ar; b, 640 Torr of Ar; c, 100 Torr of Ar, 500 Torr of $CH_4$; d, 10 Torr of Ar, 90 Torr of Xe; all with 0.01 Torr of TMBi.

above the $X_1$ $^2\Pi_{1/2}$ ground state. If this is so then the long-wavelength bands may correspond to the $(n, 0)$ and $(n + 1, 0)$ bands of the $E \leftarrow X_2$ transition.[16] In this case the $X_2-X_1$ splitting would be $>6980$ cm$^{-1}$, rather less than Bridge and Howell's estimate. An alternative explanation, that these are the $(n, 0)$ and $(n, 1)$ bands of the $E \leftarrow X_2$ transition, is unlikely since it requires that a change in spin–orbit coupling cause a change from $\omega = 692$ cm$^{-1}$ for the $X_1$ state to $\omega = 750$ cm$^{-1}$ for the $X_2$ state.

No additional spectra were observed in the presence of $N_2$, $H_2$, $CH_4$, $i$-$C_4H_{10}$, or $C_2H_4$.

In an attempt to determine the mode of formation of the highly excited species observed in emission, time-resolved emission experiments were carried out. Under all conditions the emission at 3068 Å (the Bi resonance line) exactly followed the flash profile, indicating that all processes leading to formation of excited atoms were rapid. This method of monitoring the emission was therefore abandoned.

Replacing the quartz reaction cell with a Vycor cell reduced the extent of photolysis, but strong emission was still observed from the levels previously detected.

A quartz reaction cell surrounded by a concentric, cylindrical, quartz filter jacket containing an aqueous solution of 50 mg/l. of 2,7-dimethyl-3,6-diazacyclo-hepta-1,6-diene perchlorate was also employed. This solution transmits light from 2200 to 2900 Å, has a weak absorption around 2000 Å, and absorbs very strongly from 2900 to 3500 Å with a maximum at $\sim$3200 Å. Both absorption and emission intensities were reduced only slightly by the filter. Excited-atom formation by

processes such as

$$Bi + h\nu \text{ (3068 Å)} \longrightarrow Bi^*$$

can therefore be ruled out.

It is likely, therefore, that excited atoms are produced in a multiquantum process involving intermediates such as $Bi(CH_3)_2$ and $BiCH_3$. Increasing the flash energy from 1500 to 3000 J produced an increase of a factor of 3 in the 3068-Å emission intensity. This observation is consistent with a multiquantum process since, even with a 1500-J flash, almost all of the TMBi (initially $10^{-2}$ Torr) was decomposed.

Preliminary experiments showed that added gases could have two effects on the 3068-Å emission line; they could change its shape and/or quench it. $CO_2$ and $C_2H_4$ were efficient quenchers; $CH_4$ and $i$-$C_4H_{10}$ were not.

With increasing argon pressure two distinct satellite bands, to the short-wavelength side of the 3068-Å line, became apparent. The bands displayed maxima approximately 12 and 18 Å from the line. $H_2$, $C_2H_6$, and $CH_4$ also broadened the line to shorter wavelengths. Xe (100 Torr) produced a single satellite band on the long-wavelength side of the 3068-Å line. Microdensitometer traces showing the variation in the 3068-Å line shape with the nature and pressure of the inert gas are reproduced in Figure 2.

Satellite bands have been observed[17] earlier on both sides of the Bi 3068-Å resonance line in the presence of Xe and similar bands have also been seen in other systems, notably with mercury[18,19] and alkali metal atoms.[20]

The formation of collisionally induced satellite bands close to atomic emission lines is generally attributed to the transitory formation of van der Waals molecules.[17,19] The radiative-transition probabilities for such a molecule may differ from those of the free atom and collision-induced emission from metastable atomic states has indeed been observed.[21,22]

(16) R. F. Barrow, W. J. M. Gissane, and D. Richards, Proc. Roy. Soc., Ser. A, 300, 496 (1967).

(17) D. Guy, J. Grumberg, M-O. Faucheux, and L. Herman, C. R. Acad. Sci., Ser. B, 266, 1020 (1968).

(18) A. Granzow, M. Z. Hoffman, and N. N. Lichtin, J. Chem. Phys., 51, 3621 (1969).

(19) H. E. Gunning, S. Penzes, H. S. Sandhu, and O. P. Strausz, J. Amer. Chem. Soc., 91, 7684 (1969).

(20) S.-Y. Ch'en and O. Jefimenko, J. Chem. Phys., 26, 256 (1957); O. Jefimenko and S.-Y. Ch'en, ibid., 26, 913 (1957); O. Jefimenko and W. Curtis, ibid., 27, 953 (1957).

(21) F. Mies and A. L. Smith, ibid., 45, 994 (1966).

(22) R. F. Hampson, Jr., and H. Okabe, ibid., 52, 1930(1970).
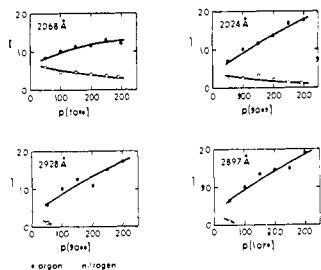
Figure 3. Variation of emission intensity from excited bismuth atoms with total pressure, 0.01 Torr of TMBi.
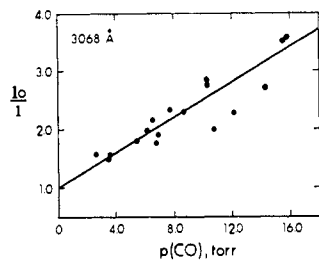


Figure 4. Variation of emission intensity from Bi(7s $^4P_{1/2}$) with added CO. Points at the intercept neglected for clarity.



Figure 5. Variation of emission intensity from Bi(7s $^4P_{1/2}$) with added $CO_2$. Points at the intercept neglected for clarity.



Figure 6. Variation of emission intensity from Bi(7s $^4P_{1/2}$) with added $CH_4$. Points at the intercept neglected for clarity.

The emission intensity in a given transition was found to increase with argon pressure, presumably because of pressure broadening. Figure 3 shows the variation with argon and nitrogen pressures of the intensities of four of the observed transitions. In all the measurements reported here, microdensitometer peak heights have been used to estimate concentrations, ignoring the contribution of satellite bands to the 3068-Å emission at higher pressures.

Quantitative quenching experiments were carried out at a total pressure of 100 Torr. At this pressure of argon, satellite band formation was negligible, and it is assumed that varying argon pressure at a constant total pressure of 100 Torr has no effect on emission intensity. The intensity was at a maximum with $10^{-2}$ Torr of TMBi and all experiments were carried out at this pressure. Because of low intensities it was only possible to study four of the states quantitatively. Results were plotted in the form $I_0/I$ vs. $p$, where $I_0$ = emission intensity in the absence of added quenching gas and $I$ = emission intensity in the presence of $p$ Torr of added quencher, $100 - p$ Torr of argon. Typical plots are shown in Figures 4–6.

For the simple system where only quenching or fluorescence is possible, the kinetics are straightforward.

$$\text{Bi}^* + \text{M} \longrightarrow \text{Bi} + \text{M} \qquad k_1$$
$$\text{Bi}^* \longrightarrow \text{Bi} + h\nu \qquad k_f$$

$$I_0/I = 1 + k_1[\text{M}]/k_f$$
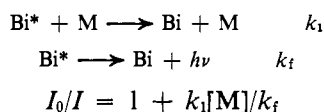
If, however, the excited state is also populated by collisional processes such as quenching of higher states, then the relationship between $I$ and [M] is complex. Plots of $I_0/I$ vs. $p$ may be curved and, if population from higher levels is more rapid than collisional deactivation, $I$ may increase with $p$.

The observed variations in line shapes with pressure imply that changes in transition probabilities are occurring and these changes may also lead to curvature in plots of $I_0/I$ vs. $p$. It is not possible to distinguish be-

tween this effect and that described in the preceding paragraph.
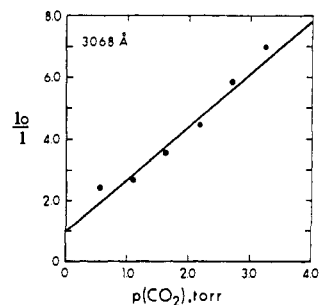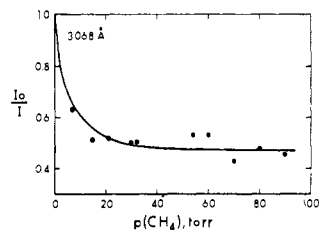
For those cases where the simple linear relationship holds, results are given in Table III in the form of $p_{1/2}$, the pressure of added quencher required to halve the emission intensity. Typically, these pressures are accurate to $\pm 30\%$, the error arising from the slight dependence of the emission intensity on the efficiency with which the cell was pumped out between flashes and from other factors, such as variations in $\gamma$ and in mixing techniques.

The $^4P_{5/2}$, $^2P_{3/2}$, and $^2P_{1/2}$ states lie in an energy region where many other states of atomic bismuth are to be found. Energy-transfer processes involving the conversion of relatively small amounts of energy to vibrational and translational modes of the quenching molecule are therefore available. The quenching of the $^2P_{1/2}$ state by $H_2$ can take place by processes such as

$$\text{Bi}(^2P_{1/2}) + H_2(v = 0) \longrightarrow \text{Bi}(?) + H_2(v = 1)$$
$$\Delta E = -624 \text{ cm}^{-1}$$

$$\text{Bi}(^2P_{1/2}) + H_2(v = 0) \longrightarrow \text{Bi}(^4S_{3/2}^0) + H_2(v = 1)$$
$$\Delta E = +119 \text{ cm}^{-1}$$
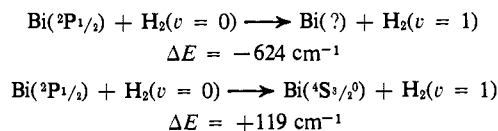
Enhancement of the 3024- and 2938-Å transitions by $H_2$ very likely occurs because of similar processes causing quenching to the upper levels of these transitions. It is not possible to estimate the importance of quenching to low-lying states in the deactivation of these species.

A different situation pertains with regard to the $^4P_{1/2}$ state observed at 3068 Å. There is no other state within 10,000 cm$^{-1}$ below this level and only the $^2P_{3/2}$ state lies within 8000 cm$^{-1}$ above. Complications brought about by quenching to this state from above are therefore reduced and any observed quenching must involve the transfer of large amounts of energy.

The only observed transition from the $^4P_{1/2}$ state other than that at 3068 Å was a weak line at 4722 Å. Quenching of this line was at least qualitatively similar to quenching of the 3068-Å line except in the case of added

**Table III.** Quenching Half-Pressures (Torr) for Excited Bismuth

| State | $6s^26p^2(^3P_0)7s$ $^4P_{1/2}$ | $6s^26p^2(^3P_2)7s$ $^4P_{5/2}$ | $6s^26p^2(^3P_2)7s$ $^2P_{3/2}$ | $6s^26p^2(^3P_1)7s$ $^2P_{1/2}$ |
|---|---|---|---|---|
| Transition | $^4P_{1/2} \rightarrow {}^4S_0$ | $^4P_{5/2} \rightarrow {}^2D_{5/2}{}^0$ | $^2P_{3/2} \rightarrow {}^2D_{5/2}{}^0$ | $^2P_{1/2} \rightarrow {}^2D_{3/2}{}^0$ |
| Wavelength | 3068 Å | 3024 Å | 2938 Å | 2898 Å |
| Xenon | ≫100 | ≫100 | 35 | Enhancement |
| Carbon monoxide | 7 | 17 | 8 | 9 |
| Nitrogen | >100 | 33 | 8 | 15 |
| Oxygen | 3 | Enhancement | 17 | 2 |
| Hydrogen | >600 | Enhancement | Enhancement | 4 |
| Methane | Enhancement | 70 | 50 | <7 |
| Ethane | Enhancement | <60 curvature | < 60 curvature | <7 |
| Ethylene | 1.0 | ~30 | ~30 | 3.0 |
| Carbon dioxide | 0.65 | 2.6 | 6 | 3.2 |

$C_2H_8$, where the 4722-Å line decreased in intensity as the 3068-Å line was enhanced. This observation, indicating an alteration in relative transition probabilities for collision-induced as compared to spontaneous emission from a given atomic state, has important implications with respect to energy-transfer studies. Additional examples of this phenomenon, which apparently has not been noted before, will be cited in the next section dealing with the quenching of excited antimony atoms.

The similarity of the intensity variations in the two lines from the $^4P_{1/2}$ state as a function of the pressure of added gases other than $C_2H_6$ and the lack of curvature in the plots for the gases which quench efficiently imply that variations in transition probabilities are not important in these cases.

Quenching of the $^4P_{1/2}$ state was not detected with 600 Torr of $H_2$ or $CH_4$. These substances are at least one order of magnitude less efficient as deactivators than $N_2$, 300 Torr of which does cause some quenching (Figure 3). The highest pressures of $C_2H_6$ and Xe employed were 100 Torr; quenching was not observed. With 600 Torr of $i$-$C_4H_{10}$, quenching did occur but no quantitative studies were carried out.

Quenching efficiencies for atomic species are customarily expressed as quenching cross sections, $\sigma^2$, defined in terms of the gas kinetic collision expression[23]

$$k_q = \sigma^2 \left(\frac{8\Pi RT}{\mu}\right)^{1/2}$$

where $k_q$ is the second-order quenching rate constant, $R$ the gas constant, $T$ the absolute temperature, and $\mu$ the reduced molecular weight of the colliding species.

At the quenching half-pressure, $p_{1/2}$, the rate of emission is equal to the rate of quenching, $k_q[M]_{1/2} = k_f$, and, therefore

$$\sigma^2 = \frac{k_f}{[M]_{1/2}} \left(\frac{8\Pi RT}{\mu}\right)^{-1/2}$$

where $[M]_{1/2}$ is the half-quenching concentration corresponding to $p_{1/2}$.

A value of 5.9 nsec has recently been obtained[24] for the lifetime of the 7s $^4P_{1/2}$ state of bismuth. Since it is estimated[24] that 97% of the emission from this state is concentrated in the 3068-Å line, we have used the reciprocal of the measured lifetime as $k_f$ in the calculation of quenching cross sections for Bi. The results of these calculations are given in Table IV, together with some

**Table IV.** Quenching Cross Sections[a]

| | $Hg(^3P_1)^b$ 300°K | $Tl(7s\ ^2S_{1/2})^c$ 1400°K | $Pb(7s\ ^3P_1{}^0)^d$ 1400°K | $Bi(7s\ ^4P_{1/2})^e$ 300°K |
|---|---|---|---|---|
| | | | $\Delta E$, cm⁻¹ | |
| | 39412 | 26478 | 35287 | 32588 |
| $H_2$ | 9.8 | <0.03 | 0.4 | <0.15 |
| $O_2$ | 23 | 13.2 | 15 | 110 |
| $N_2$ | 0.35 | 6.4 | 5.7 | <3.5 |
| CO | 7 | 13.6 | 13 | 46 |
| $CO_2$ | 2.5 | 32.5 | 32.5 | 620 |
| Xe | | | | ≪6 |
| $CH_4$ | 0.06 | | | <0.5 |
| $C_2H_6$ | 0.4 | | | <0.6 |
| $C_2H_4$ | 42 | | | 330 |

[a] Cross sections are given in units of $10^{-16}$ cm². $\Delta E$ = energy transferred assuming ground-state atoms are produced. [b] Cross-section values taken from A. J. Yarwood, O. P. Strausz, and H. E. Gunning, *J. Chem. Phys.*, **41**, 1705 (1964); K. Yang, *J. Amer. Chem. Soc.*, **89**, 5344 (1967). [c] Values from ref 8. [d] Values from ref 9. [e] This work. Data for Bi are upper limits calculated on the assumption of zero imprisonment of resonance radiation.

quenching cross sections for other species which are included for comparison.

Since no account has been taken of imprisonment of resonance radiation, the data for Bi in Table IV are an upper limit. No correction for imprisonment was made because of the variation in the concentration of the absorbing species with time. This variation was the same in all cases studied and, therefore, the relative magnitudes of the quoted cross sections are correct.

If we assume that all of the TMBi is converted to ground-state bismuth atoms, the atom concentration is of the order of $3 \times 10^{14}$ atoms/cm³. At this concentration of mercury and under similar conditions the radiative lifetime of $Hg(^3P_1)$ is increased by imprisonment from its zero-pressure value of $1.1 \times 10^{-7}$ to $5 \times 10^{-6}$ sec.[25] Since the absorption coefficient is larger, an even larger effect is expected in the case of bismuth.[26]

**(b) TMSb.** The uv absorption spectrum of TMSb consists of a continuum between 2100 and 2400 Å with a maximum at 2250 Å ($\epsilon$ 1 $\times$ 10⁴ l. mol⁻¹ cm⁻¹).

The species detected in absorption following the flash photolysis of TMSb (1–0.01 Torr) with 200 Torr of argon as diluent are listed in Table V. The states of atomic antimony which were detected in either absorption or emission are shown on the energy-level diagram given in Figure 7.[18] Basco and Yee[27] have reported the

(23) Reference 1, p 73.
(24) P. T. Cunningham and J. K. Link, *J. Opt. Soc. Amer.*, **47**, 1000 (1967).

(25) Reference 1, p 64.
(26) The time-resolved emission experiments show that $k_f$ > 1 × 10⁶ sec⁻¹, hence a lower limit of ~10³ less than the values of Table IV can be placed on the bismuth quenching cross sections.
(27) N. Basco and K. K. Yee, *Nature (London)*, **216**, 998 (1967).

**Table V.** Species Observed in Absorption in Flashed TMSb

| Species | | | Transition, Å | Conditions under which observed | Time to max intensity, $\mu$sec | Time species persists, $\mu$sec | Comments |
|---|---|---|---|---|---|---|---|
| Sb | $^4S_{3/2}^0$ | $^4P_{1/2}$ ← | 2311 | All | 30 | 200 | Also at 2175 Å |
| Sb | $^2D_{3/2}^0$ | $^2P_{1/2}$ ← | 2598 | All | 30 | 75 | Also many other transitions |
| Sb | $^2D_{5/2}^0$ | $^2P_{3/2}$ ← | 2528 | All | 30 | 75 | Also many other transitons |
| Sb | $^2P_{1/2}^0$ | $^2P_{3/2}$ ← | 3030 | All | 30 | 75 | Also many other transitions |
| Sb | $^2P_{3/2}^0$ | $^2P_{3/2}$ ← | 3233 | All | 30 | 75 | Also many other transitions |
| Sb$_2$ | $X'\Sigma_g^+$ | ← | <2100 | All | 100 | 250 | Nakamura and Shidei's System III[29] |
| Sb$_2$ | $X'\Sigma_g^+$ F | ← | 2200–2270 | All | 100 | 250 | Nakamura and Shidei's System II[29] |
| Sb$_2$ | $X'\Sigma_g^+$ D | ← | ~2900 | All | 100 | 250 | |
| CH$_3$ | | | 2160 | All | 30 | 100 | |
| ? | | | 2285 | All | 10 | 50 | Diffuse, 10 Å wide |
| ? | | | 2590 | All | 10 | 50 | Diffuse, 20 Å wide; same carrier as 2285-Å band? |
| ? | | | 2411 | All | 20 | 150 | Weaker band 1 Å to short wavelength |
| ? | | | 2475 | All | 20 | 100 | Weaker band 2 Å to short wavelength; same carrier as 2411-Å band? Different time dependence owing to low intensity? |

observation of emission from excited atoms in flashed antimony hydride, but no quenching measurements were performed.
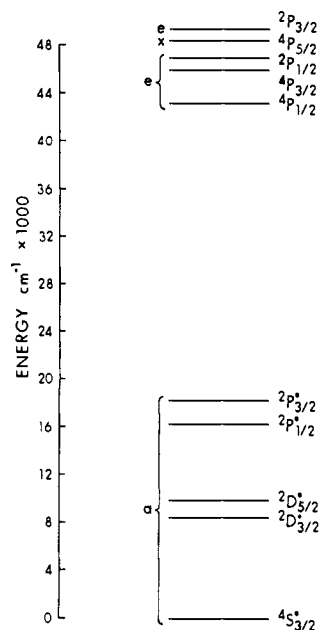


Figure 7. Atomic energy level diagram for antimony: a, states observed in absorption; e, states observed in emission; x, not observed.

The absorption spectrum of Sb$_2$ has been observed in antimony vapor by Naudé[28] and by Nakamura and Shidei.[29] These authors give conflicting vibrational analyses for the D–X system around 2900 Å, but that of Naudé is preferred because of the agreement between his calculated and experimentally determined isotope splittings. The bands we observe are the $(n, 0)$ and

(28) S. M. Naudé, *S. Afr. J. Sci.*, **32**, 103 (1935).
(29) G. Nakamura and T. Shidei, *Jap. J. Phys.*, **10**, 11 (1935).

$(m, 2)$ where $n = 14$–9 and $m = 17$–11 according to Naudé, and $n = 6$–1, $m = 9$–3 according to Nakamura and Shidei.

We could not detect vibrational relaxation of Sb$_2$ during its lifetime and we conclude that we are observing a Boltzmann distribution of vibrational energies. The relative magnitudes of the Franck–Condon factors for these transitions must then be $f_{v''=2} > f_{v''=0} \gg f_{v''=1}$ in order to explain the observed intensities.

No additional spectra were recorded in the presence of H$_2$, CH$_4$, C$_2$H$_4$, CO, or CO$_2$. A dark reaction between TMSb and O$_2$ precluded the possibility of work with this gas.
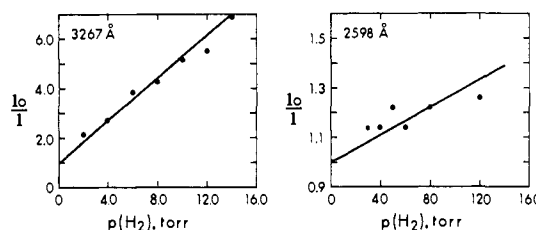


Figure 8. Variation of emission intensity from Sb(6s $^2P_{1/2}$) with added H$_2$. Points at the intercept neglected for clarity.

Four atomic lines were observed in emission with sufficient intensity for quantitative work. The upper states involved were the 6s $^2P_{3/2}$ state observed at 2529 and 3233 Å and the 6s $^2P_{1/2}$ state at 2598 and 3268 Å. Quenching experiments were carried out with 0.05 Torr of TMSb and 200 Torr of argon as inert diluent and the results plotted in the form $I_0/I$ vs. $p$. Typical plots are shown in Figures 8–10. The data are compiled in Table VI in the form of quenching half-pressures, $p_{1/2}$, where these could be measured. The accuracy of these results is $\pm 30\%$, the sources of error being similar to those discussed in the case of bismuth.

A source of complications in the interpretation of the data of Table VI is the 6s $^4P_{5/2} \rightarrow$ $^2D_{5/2}^0$ transition at

**Table VI.** Quenching Half-Pressures (Torr) for Excited Antimony

| State | $5s^25p^2(^3P_2)6s\ ^2P_{3/2}$ | $5s^25p^2(^3P_2)6s\ ^2P_{3/2}$ | $5s^25p^2(^3P_1)6s\ ^2P_{1/2}$ | $5s^25p^2(^3P_1)6s\ ^2P_{1/2}$ |
|---|---|---|---|---|
| Transition | $^2P_{3/2} \rightarrow\ ^2D_{3/2}^0$ | $^2P_{3/2} \rightarrow\ ^2P_{3/2}^0$ | $^2P_{1/2} \rightarrow\ ^2D_{3/2}^0$ | $^2P_{1/2} \rightarrow\ ^2P_{1/2}^0$ |
| Wavelength | 2529 Å | 3233 Å | 2598 Å | 3268 Å |
| Xenon | 75 | 75 | Enhanced | Enhanced |
| Carbon monoxide | 4 | 9 | 35 | 1 |
| Nitrogen | 12 | 12 | 35 | 35 |
| Hydrogen | 10 | 4 | >200 | 2.5 |
| Methane | Enhanced | 1 | 4 | 4 |
| Ethane | 6 | 0.3 | 2.5 | 2.5 |
| Ethylene | 6 | 0.5 | Enhanced | 0.2 |
| Carbon dioxide | 3 | 3 | 2 | 3 |

2598 Å which could account for the differences in apparent quenching rates between the 2598- and the 3268-Å line. However, the $^4P_{5/2} \rightarrow\ ^2D_{3/2}^0$ transition at 2510.5 Å was not detected under any of the conditions used and we conclude that emissions from the $^4P_{5/2}$ state are of low intensity and are not important in this study.
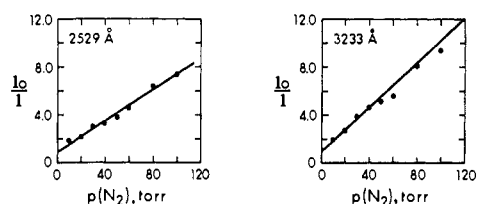


Figure 9. Variation of emission intensity from Sb(6s $^2P_{3/2}$) with added $N_2$. Points at the intercept neglected for clarity.
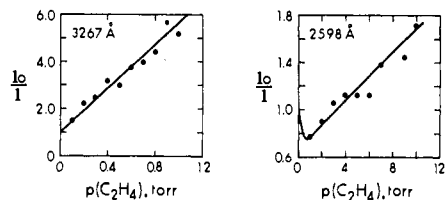


Figure 10. Variation of emission intensity from Sb(6s $^2P_{1/2}$) with added $C_2H_4$. Points at the intercept neglected for clarity.

The variation of relative intensities of transitions from the same state, first noted with bismuth, is demonstrated more clearly in the case of antimony. In Figure 11 microdensitometer traces showing the effect of added $H_2$ on the $^2P_{1/2}$ lines are presented. The shape of the 2598-Å line is affected by $H_2$ but the 3268-Å line is quenched much more efficiently. Similar effects occur with CO and $C_2H_4$ and, for the 2528- and 3233-Å lines, with $H_2$, CO, $CH_4$, $C_2H_6$, and $C_2H_4$.

Distinct satellite bands were not observed on any of the atomic lines but, as Figure 11 shows, line shapes did vary with added gas pressure. The absence of satellite bands is probably due to the low intensities of the antimony transitions as compared to the 3068-Å bismuth resonance line.

When cross sections for the deactivation of excited atoms are determined by studies of the quenching of atomic emissions it is assumed that, after correction for imprisonment, the probability of the observed transition remains constant. The observation of collisionally induced emission from metastable atomic states[21,22] shows that this is not necessarily the case. The results of this investigation demonstrate that collisional effects may cause variations even in relative transition proba-

bilities from the same state. Therefore, in quantitative quenching experiments where more than one terminating emission process is available, the possible role of this effect should not be overlooked.
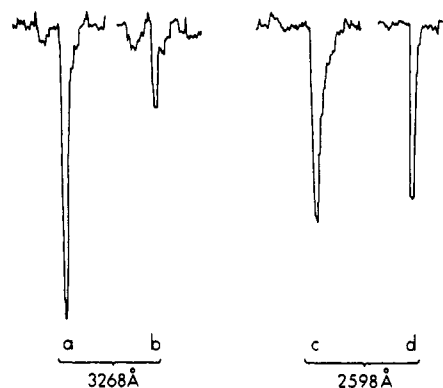


Figure 11. Effect of added $H_2$ on emission from Sb(6s $^2P_{1/2}$) at 3268 and 2598 Å: a and c, 200 Torr of Ar; b and d, 200 Torr of Ar, 10 Torr of $H_2$; all with 0.05 Torr of TMSb.

The mechanisms of the quenching processes are complex and their interpretation is made difficult by lack of information concerning the products. The observation of BiO in the TMBi–$CO_2$ system requires that oxygen abstraction be a principal mode of quenching. The reactions of $^2P_J$ state atoms with $CO_2(X\ ^1\Sigma^+)$ to produce BiO(X $^2\Pi$) and CO(X $^1\Sigma^+$) are symmetry and spin allowed, but the similar reactions of Bi($^4P_J$) states are spin forbidden. Production of the lowest quartet state, BiO(B $^4\Sigma^-$), is energetically unlikely. Heavy-atom effects may facilitate the spin inversion, however, and allow BiO(X $^2\Pi$) production. Reactions of $^4P_J$ + $^2P_J$ atoms with $O_2(X\ ^3\Sigma_g^-)$ to yield BiO(X $^2\Pi$) and O($^3P$, $^1D$) are spin allowed and energetically feasible.

The failure to observe SbH or BiH in $H_2$ and hydrocarbon systems is surprising, since the hydrogen abstraction would be symmetry and spin allowed and energetically possible, and also since some states are quenched with relatively high efficiencies.

In the case of Xe, $N_2$, and CO, transient complex formation must be invoked. Quenching can then occur if favorable potential surface crossings are available. Spin inversion at the crossover will be facilitated by heavy-atom perturbations.

Further studies are in progress.